electron correlation, the application of which is presently under investigation.

Conclusion

The spectromagnetic properties of the $[Co_6(\mu_3\text{-}S)_8(PEt_3)_6]BPh_4$ cluster have been found to be rather complicated. At room temperature, the cluster is EPR silent and shows a rather exceptional well-resolved ^1H NMR spectrum. These properties suggest a delocalization of the unpaired electron over the whole molecule, even if the cobalt centers are crystallographically nonequivalent, which results in short relaxation times and a small spin density on the phosphorus atoms. The 4.2 K single-crystal EPR spectra are typical of a low-spin cobalt(II) complex, which can be formed if the unpaired electron localizes upon a decrease in temperature, and the angular dependence of the peak-to-peak line width of the EPR signal can indicate the existence of a magnetic interaction between the magnetic clusters, which are arranged in the solid state in an alternating linear chain in the *bc* plane. The observed magnetic behavior agrees with this interpretation. The low symmetry of the complex, while aiding us in the measurement of the molecular **g** tensor, prevented any deeper investigation of the intercluster interactions; also, the absence of a resolved hyperfine and/or superhyperfine splitting prevented a direct measurement of the localization of the unpaired electron. Since the extent of localization in mixed-valence complexes is the subject of active research and the above results show that magnetic and EPR measurements can yield useful information in this area, higher symmetry clusters are now under investigation.

The phosphine ligands prevent the formation of an extended structure with strong bonding interactions between the clusters, which have been observed in other oligonuclear compounds and are responsible for peculiar physical properties, but in a sense they modulate the electronic structure of the clusters through the creation of an energy gap inside the metal d band, influencing their redox and electron-transport properties. An analysis based on spin-unrestricted Xα–SW calculations[19] is in progress to study the relative stabilities of the degrees of oxidation of the cluster upon varying the number of electrons on the metals and to investigate the resulting spin structures.

Acknowledgment. Thanks are expressed to Prof. O. Kahn, Université de Paris Sud, for the magnetic measurements; to Prof. M. Verdaguer, Université P. et M. Curie, Paris, for his kind hospitality and helpful discussions; to Prof. D. Gatteschi, Università di Firenze, for his encouragement and suggestions; and to Mr F. Cecconi, for assistance in the chemical manipulations.

Registry No. $[Co_6(\mu_3\text{-}S)_8(PEt_3)_6]BPh_4$, 81289-54-5.

Contribution from the Department of Chemistry, University of Alberta, Edmonton, Alberta, Canada T6G 2G2

Kinetic Study of the Reaction of 3-Methylascorbic Acid with Aqueous Iron(III)

M. J. Sisley and R. B. Jordan*

Received December 26, 1991

The reactions of aqueous iron(III) with 3-methylascorbic acid (3-MeAsH) have been studied in dilute acid with iron(III) in excess in 1.0 M $LiClO_4/HClO_4$ at 25 °C. There is initial formation of a violet complex followed by much slower fading of the color. The formation of the violet color was studied by stopped-flow, and the iron(III) and H^+ dependence of the rate are consistent with the reaction of $(H_2O)_5FeOH^{2+}$ and 3-MeAsH with a rate constant of $(2.2 \pm 0.05) \times 10^3$ M^{-1} s^{-1}) to form $(H_2O)_5Fe(3\text{-}MeAs)^{2+}$. The slow step, which involves oxidation of 3-MeAsH and formation of iron(II), is strongly inhibited by iron(II), and the kinetics of the reaction have been studied with a pseudo-first-order excess of Fe^{2+}, with $[Fe^{2+}] \approx$ [3-MeAsH] and with no initial Fe^{2+}. For the latter two conditions, the absorbance–time profiles have been fitted by numerical integration of the appropriate second-order rate law. The oxidation follows two parallel pathways whose contributions depend on the $[Fe^{2+}]$. One pathway has an $[Fe^{2+}]^{-1}$ dependence and has an irreversible step prior to the transfer of the second electron. The other pathway, with an $[Fe^{2+}]^{-2}$ dependence, is analogous to that found previously for 1,2-dihydroxybenzoic acid. The analysis yields specific rate constants for the first electron transfer of 0.88 and 64 M^{-1} s^{-1} for $Fe(OH_2)_6^{3+}$ and $(H_2O)_5FeOH^{2+}$, respectively, and rate constant ratios for several intermediate steps.

Introduction

A recent study[1] of the reaction of aqueous iron(III) with ascorbic acid (**1**) has confirmed earlier observations[2] of the formation

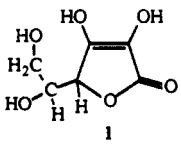

1

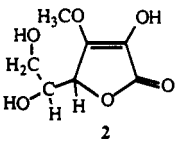

2

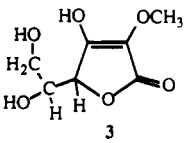

3

of a transient blue iron(III)–ascorbate intermediate and shown that this intermediate is oxidized by a second iron(III). It was also found[1] that the rate of formation of the blue species is unusually fast for substitution on $Fe(OH_2)_6^{3+}$ or $Fe(OH_2)_5OH^{2+}$. Observations during early preparative work[3] on the methyl derivatives of ascorbic acid indicated that 3-methylascorbic acid (**2**) (3-MeAsH) forms a more persistent blue complex than ascorbic acid, but the 2-methyl derivative (**3**) does not form a colored complex. These observations must have some relevance to the mode of coordination of ascorbate to aqueous iron(III). The fact that 3-methylascorbic acid is a much weaker acid ($pK_a = 7.9$)[4] than ascorbic acid ($pK_a = 4$) may also be helpful in differentiating the reactivity of the ionized forms in these systems. The acidity difference is consistent with the conclusion of Berger[5] that the 3-OH proton is the most acidic in ascorbic acid. However, it is then somewhat unexpected that the 3-methyl derivative also forms a blue iron(III) complex.

Some effort has been made to elucidate the organic products of the oxidation of 3-MeAsH, especially to determine if the methyl group is lost. Therefore it is pertinent to review briefly the information on the oxidation products of ascorbic acid. This problem has received considerable attention, but the literature is somewhat conflicting. Tolbert and Ward[6] have provided a review and new

(1) Xu, J.; Jordan, R. B. *Inorg. Chem.* **1990**, *29*, 4180.
(2) Laurence, G. S.; Ellis, K. J. *J. Chem. Soc., Chem. Commun.* **1972**, 1676. Keypour, H.; Silver, J.; Wilson, M. T.; Hamed, M. Y. *Inorg. Chim. Acta* **1986**, *125*, 97. Martinez, P.; Zulaga, J.; Uribe, D. *Z. Phys. Chem. (Munich)* **1987**, *268*, 105. Hynes, M. J.; Kelly, D. F. *J. Chem. Soc., Chem. Commun.* **1988**, 849.
(3) Haworth, W. N.; Hirst, E. L.; Smith, F. *J. Chem. Soc.* **1934**, 1556. Haworth, W. N.; Hirst, E. L. *Helv. Chim. Acta* **1934**, *17*, 520.
(4) Lu, P. W.; Lillard, D. W., Jr.; Seib, P. A.; Kramer, K. J.; Liang, Y.-T. *J. Agric. Food Chem.* **1984**, *32*, 21.
(5) Berger, S. *Tetrahedron* **1977**, *33*, 1587.

0020-1669/92/1331-2137$03.00/0

Scheme I

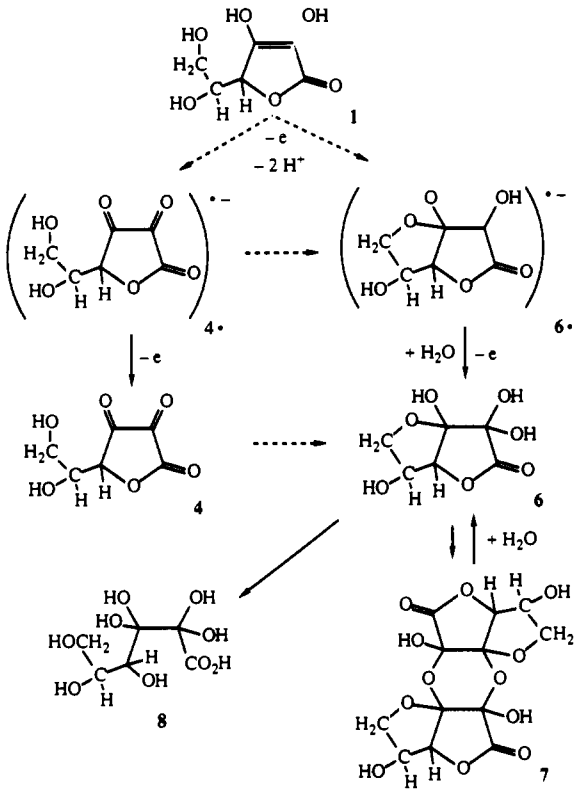

information to clarify the situation. It is generally agreed that the oxidation product of ascorbic acid, commonly called dehydroascorbic acid (DHA), does not have the diketone structure (**4**)

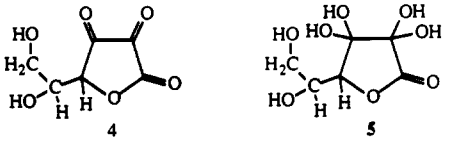

and is most commonly shown as the hydrate (**5**). However the NMR evidence shows that DHA is not (**5**) but rather has the bicyclic structure (**6**).

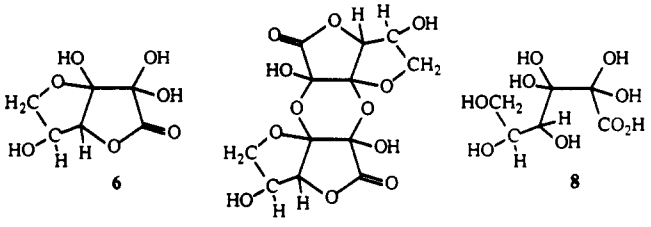

Some confusion has arisen because the dimer (**7**), whose structure was determined by Hvoslef,[7] is normally the source of oxidized ascorbic acid for NMR studies. Hvoslef and Pedersen[8] found that **7** in DMF or DMSO dissociates readily to **6** if water is added. Therefore the spectrum assigned to **7** by Berger[5] and Matusch[9] is probably **6**. A further complication is that **6** hydrolyzes to diketogulonic acid (**8**) which decarboxylates to 3,4,5-trihydroxy-2-ketovaleraldehyde. Both Berger and Matusch assigned the stable iodine oxidation product to **5**, but the spectra actually appear to be that of **8**. Kang et al.[10] also found that the species derived from **6** and assigned to **5** by Hvoslef and Pedersen is actually **8**. There does not appear to be any concrete evidence for **5** as a significant species in solutions of dehydroascorbic acid.

The NMR spectra of species derived from **7** indicate the thermodynamically stable products but may not reflect the immediate oxidation products. The situation with regard to the oxidation is summarized in Scheme I.

The nature and structure of the radical from one-electron oxidation was assigned by Laroff et al.[11] to **4**•, and the next electron loss would give **4**. However, Sapper et al.[12] have proposed the bicyclic structure **6**• because the hyperfine coupling to the CH_2 protons (0.19 G) is larger than that for the CH proton (0.06 G) and because the derivatives with the side chain acetylated (to prevent cyclization) do not show hyperfine coupling to the CH_2 protons. However, Kirino and Kwan[13] studied the oxidation by $Ti^{3+} + H_2O_2$ in an ESR flow cell and found that the 5,6-isopropylidene derivative of ascorbic acid, which cannot cyclize, gives the same ESR spectrum as ascorbic acid. They suggest that the hyperfine coupling to the CH_2 protons is due to a spin polarization mechanism rather than cyclization. Kirino and Kwan also note that 3-MeAsH does not give an ESR spectrum under their conditions. Cabelli and Bielski[14] used pulsed radiolysis to study the decomposition kinetics of the 3-MeAsH radical but did not investigate the decomposition products.

There is some further information on the overall course of the oxidation. Matusch[9] observed an intermediate in the iodine oxidation in anhydrous DMSO which was assigned to **4** and which cyclizes and hydrates to give **6** (originally assigned as **7**) and finally yields what now appears to be **8**. This seems to be the most direct evidence that **4** is on the reaction pathway, and Tolbert and Ward[6] have suggested a detailed mechanism for the acid-catalyzed transformation of **4** to **6**. The apparent detection of **4** by Matusch as the iodine oxidation product in DMSO indicates that cyclization does not occur in the radical, but the situation could be different in water if the diketone radical hydrates and cyclizes more rapidly than it is oxidized. Some indirect information on the cyclization can be obtained from the observations of Kwan and Foote[15] that the hydroperoxide **9** cyclizes to **10** with a half-time which seems

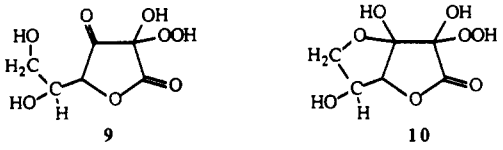

to be ~5 h at −78 °C in methanol. This leads to $k \approx 10\ s^{-1}$ at 25 °C, assuming $\Delta S^{\ddagger} = 0$. It seems probable that the cyclization of oxidized radical cation intermediates would be much faster than this. Therefore, the possibility remains that the reaction pathway is complex and depends on competition between cyclization and oxidation of **4**• and will vary with the concentration and nature of the oxidizing agent.

The structure of the ascorbate radical is of importance for analyses of the reaction rates in terms of Marcus' theory. In 1981, Creutz[16] mentioned the problems concerning the cyclic species and Marcus theory calculations before there was a preponderance of evidence that dehydroascorbate is bicyclic. Despite this warning, there continue to be attempts[17,18] to calculate the electron exchange rate of ascorbate and its oxidized radical on the basis of Marcus theory correlations. Marcus theory correlations for ascorbate

(6) Tolbert, B. M.; Ward, J. B. In *Ascorbic Acid: Chemistry, Metabolism and Uses*; Seib, P. A., Tolbert, B. M., Eds.; Advances in Chemistry Series, Vol. 200, American Chemical Society: Washington, DC, 1982; pp 101–123.
(7) Hvoslef, J. *Acta Crystallogr.* **1972**, *28B*, 916.
(8) Hvoslef, J.; Pedersen, B. *Acta Chem. Scand.* **1979**, *33B*, 503.
(9) Matusch, R. *Z. Naturforsch.* **1976**, *32b*, 562.
(10) Kang, S.-O.; Sapper, H.; Lohman, W. *Z. Naturforsch.* **1982**, *37c*, 1064.
(11) Laroff, G. P.; Fessenden, R. W.; Schuler, R. H. *J. Am. Chem. Soc.* **1972**, *94*, 9062.
(12) Sapper, H.; Pleyer-Weber, A.; Lohman, W. *Z. Naturforsch.* **1982**, *37c*, 129.
(13) Kirino, Y.; Kwan, T. *Chem. Pharm. Bull.* **1972**, *20*, 2651.
(14) Cabelli, D. E.; Bielski, H. *J. Radiat. Phys. Chem.* **1984**, *23*, 419.
(15) Kwan, B.-Y.; Foote, C. S. *J. Am. Chem. Soc.* **1988**, *110*, 6582.
(16) Creutz, C. *Inorg. Chem.* **1981**, *20*, 4449.
(17) Macartney, D.; Sutin, N. *Inorg. Chim. Acta* **1983**, *74*, 221. Drury, W. D.; DeKorte, J. M. *Inorg. Chem.* **1983**, *22*, 121. Hoddenbagh, J. M. A.; Macartney, D. H. *J. Chem. Soc., Dalton Trans.* **1990**, 615. Kelley, P. M.; Jalukar, V. J.; Njus, D. *J. Biol. Chem.* **1990**, *265*, 19409. Jalukar, V.; Kelley, P. M.; Njus, D. *J. Biol. Chem.* **1991**, *266*, 6878.
(18) Bänsch, B.; Martinez, P.; Uribe, D.; Zuluaga, J.; van Eldik, R. *Inorg. Chem.* **1991**, *30*, 4555.

Scheme II

$$Fe(OH_2)_6^{3+} + 3\text{-MeAs}^- \underset{k_{-1}}{\overset{k_1}{\rightleftharpoons}} (H_2O)_5Fe(3\text{-MeAs})^{2+} + H_2O$$

$$Fe(OH_2)_5(OH)^{2+} + 3\text{-MeAs}^- \underset{k_{-2}}{\overset{k_2}{\rightleftharpoons}} (H_2O)_5Fe(3\text{-MeAs})^{2+} + OH^-$$

$$Fe(OH_2)_5(OH)^{2+} + 3\text{-MeAsH} \underset{k_{-3}}{\overset{k_3}{\rightleftharpoons}} (H_2O)_5Fe(3\text{-MeAs})^{2+} + H_2O$$

$$Fe(OH_2)_6^{3+} + 3\text{-MeAsH} \underset{k_{-4}}{\overset{k_4}{\rightleftharpoons}} (H_2O)_5Fe(3\text{-MeAs})^{2+} + H_3O^+$$

oxidation which use thermodynamic parameters that relate ascorbic acid to **6**• and **6** may still appear to work, but they will underestimate the self-exchange rate if the bicyclic radical is more stable than its monocyclic parent.

Results and Discussion

The overall course of the reaction of 3-MeAsH with aqueous iron(III) is similar to but slower than that for ascorbic acid.[1] There is initial formation of a violet complex with an absorbance maximum at about 550 nm. Then the violet color fades in a redox process to produce iron(II). The fading is inhibited by iron(II) in both cases.

Kinetics of Complexation. The formation of the violet complex was followed at 580 nm with iron(III) in large excess over 3-MeAsH. The concentration conditions were chosen to avoid the formation of higher iron(III)–3-MeAs complexes and reactions of radical intermediates with ascorbate species. The absorbance changes are in the range of 0.3 absorbance units and vary as expected with the iron(III) and H^+ concentration. The reagent concentrations and kinetic results are summarized in Table I. The pseudo-first-order rate constants increase with increasing iron(III) concentration and decreasing H^+ concentration and are unaffected by iron(II).

The standard reaction scheme for substitution is shown in Scheme II. This leads to the pseudo-first-order rate constant given by

$$k_{obsd} = [k_2K_mK_a[H^+]^{-1} + (k_1K_a + k_3K_m) + k_4[H^+]]\left\{\frac{[FeOH_2^{3+}]}{[H^+]} + \frac{1}{K_f}\right\} \quad (1)$$

where K_a is the acid dissociation constant of 3-MeAsH, K_m[19] is the hydrolysis constant of $Fe(OH_2)_6^{3+}$, $[FeOH_2^{3+}]$ is the concentration of $Fe(OH_2)_6^{3+}$ calculated after taking account of hydrolysis and dimerization of aqueous iron(III), and $[H^+]$ is the concentration corrected for the same processes. The K_f is defined by

$$K_f = k_4/k_{-4} = [Fe(3\text{-MeAs})^{2+}][H^+]/[FeOH_2^{3+}][3\text{-MeAsH}]$$

Trial analyses reveal that the only significant terms in eq 1 involve $(k_1K_a + k_3K_m)$ and K_f, and least-squares fitting gives values of 3.51 ± 0.08 s^{-1} and 0.51 ± 0.16, respectively. The observed and calculated rate constants are compared in Table I.

The much greater substitution reactivity of ascorbic acid can be seen directly from its value of $(k_1K_a + k_3K_m) = 74$ (16 °C), compared to 3.5 (25 °C) for 3-MeAsH. The determination of the dominant term in $(k_1K_a + k_3K_m)$ can only be made on the basis of rate constant comparisons. If k_1K_a is the dominant term, then $k_1 \approx 2.8 \times 10^8$ M^{-1} s^{-1}, which seems quite unreasonable since anions reacting with $Fe(OH_2)_6^{3+}$ typically have rate constants in the range of 10–100 M^{-1} s^{-1}. If k_3K_m is the dominant term, then $k_3 \approx 2.2 \times 10^3$ M^{-1} s^{-1}, and this is a normal value for substitution on $Fe(OH_2)_5(OH)^{2+}$. For ascorbic acid, this type of analysis gives an ambiguous result because K_m is not so different from K_a, but the results with squaric acid[20] suggest that the correct assignment gives $k_3 = 7.4 \times 10^4$ M^{-1} s^{-1} (16 °C) for ascorbic acid.

Table I. Kinetic Results for the Faster Reaction of Iron(III) and 3-Methylascorbic Acid, at 25 °C, $\mu = 1.0$ M ($HClO_4/LiClO_4$)[a]

$10^2[Fe^{3+}]_i$, M	$10^2[H^+]_i$, M	$10^2[FeOH_2^{3+}]_f$, M	$10^2[H^+]_f$, M	k, s^{-1} obsd	k, s^{-1} calcd
4.20	1.00	3.14	2.26	12.2	11.7
4.20	1.00	3.14	2.26	12.1	11.7
4.20	1.00	3.14	2.26	12.3	11.7
4.20[b]	1.00	3.14	2.26	12.0	11.7
4.20[c]	1.00	3.28	2.07	13.9	12.4
4.20[d]	1.00	3.14	2.26	12.3	11.7
4.20[e]	1.00	3.14	2.26	12.3	11.7
3.50[c]	1.00	2.59	2.08	11.7	11.2
3.50	1.00	2.73	1.91	12.9	11.9
2.80	1.00	2.06	1.90	10.6	10.7
2.80[c]	1.00	2.04	1.49	11.6	11.7
2.10	1.00	1.54	1.71	9.98	10.0
1.40	1.00	1.02	1.50	9.47	9.27
1.40	1.00	1.02	1.50	9.29	9.27
1.40[b]	1.00	1.02	1.50	9.32	9.27
4.20	2.00	3.36	3.00	9.65	10.8
3.50	2.00	2.80	2.84	9.01	10.3
2.80	2.00	2.25	2.68	8.80	9.82
2.10	2.00	1.70	2.50	8.84	9.26
1.40	2.00	1.15	2.32	8.03	8.61
4.20	5.00	3.77	5.25	8.55	9.27
2.80	5.00	2.56	5.31	8.24	8.56
1.40	5.00	1.31	5.13	8.07	7.77
1.40	5.00	1.31	5.13	8.53	7.77
1.00	5.00	0.944	5.08	8.12	7.52
0.750	5.00	0.712	5.06	7.93	7.37

[a] Solutions contain $(7.04–7.27) \times 10^{-4}$ M 3-methylascorbic acid, and observations are at 580 nm unless otherwise indicated; the concentrations are the initial (i) stoichiometric values and the final (f) values after correction for hydrolysis of iron(III). [b] Solution also contained 1.4×10^{-2} M iron(II) perchlorate. [c] 3-Methylascorbate in water was mixed with iron(III) in 0.020 M $HClO_4$; this gives less μ-dihydroxy-iron(III) dimer than when solutions of equal acidity are mixed. [d] Observed at 620 nm. [e] Observed at 540 nm.

It is possible to determine upper limits on the other rate constants because $k_2K_aK_m[H^+]^{-1} + k_4[H^+]$ must be $\ll 3.5$. From the lowest acidity studied of 0.015 M, one obtains $k_2 < 2.6 \times 10^9$ M^{-1} s^{-1}, and from the highest acidity of 0.055 M, $k_4 < 64$ M^{-1} s^{-1}. Since k_2 for other systems is in the range of 10^3–10^4, it is not unexpected that this term is not contributing for 3-MeAsH under our conditions. As discussed previously by Xu and Jordan,[1] k_4 is typically <10 M^{-1} s^{-1}, but ascorbic acid is unusual in having $k_4 = 5.5 \times 10^3$ M^{-1} s^{-1} (16 °C). Clearly, 3-MeAsH is much less reactive with $Fe(OH_2)_6^{3+}$ than ascorbic acid. It was suggested[1] that ascorbic acid might be unusually reactive because the large bite distance between the oxygens (~3.0 Å) allows it to form a favorable precursor complex. The presence of a methyl group on one of these oxygens may provide steric problems for such a precursor complex.

Products and Kinetics of the Oxidation Stage. Under anaerobic conditions, the violet color of solutions of iron(III) and 3-MeAsH slowly fades to colorless. This change is accompanied by formation of 2 mol of iron(II) per mole of 3-MeAsH, as shown qualitatively and quantitatively by adding *o*-phenanthroline to give the characteristic red color of the iron(II)–phenanthroline complex. The rate of disappearance of the violet color is strongly inhibited by iron(II) even at the millimolar level.

Because some of these kinetic runs extend over many hours, the hydrolytic stability of 3-MeAsH was examined. After 85 h at ambient temperature, the ^{13}C spectrum of 0.01 M 3-MeAsH in 0.012 M $HClO_4$ showed no change and no evidence of methanol. The CD spectrum serves to differentiate 3-MeAsH and ascorbic acid.[21] The spectrum of 1.5×10^{-4} M 3-MeAsH in either 0.01 or 0.05 M $HClO_4$ at ambient temperature was unchanged over a 4 day period. It was also shown that passage of such a solution

(19) Baes, C. F.; Messmer, R. E. *The Hydrolysis of Cations*; Wiley: New York, 1976; Chapter 10.5. The value of $K_m = 1.62 \times 10^{-3}$ M in 1.0 M $NaClO_4$ has been used.

(20) Sisley, M. J.; Jordan, R. B. *Inorg. Chem.* **1991**, *30*, 2190.

(21) The CD spectrum of 3-MeAsH shows a positive extremum near 240 nm and a negative extremum near 215 nm, while ascorbic acid has a negative extremum near 240 nm.

Table II. Kinetic Results for the Slower Reaction of Iron(III) and 3-Methylascorbic Acid, at 25 °C, μ = 1.0 M ($HClO_4/LiClO_4$)[a]

$10^2[Fe^{3+}]_i$, M	$10^2[H^+]_i$, M	$10^2[Fe^{2+}]$, M	$10^2[FeOH_2^{3+}]_f$, M	$10^2[H^+]_f$, M	10^5k,[b] s^{-1} obsd	10^5k,[b] s^{-1} calcd
1.40	2.00	3.00	1.20	2.20	1.18	1.13
1.40	2.00	1.95	1.20	2.20	1.88	1.73
1.40	2.00	1.05	1.20	2.20	3.11	3.22
1.40	2.00	0.450	1.20	2.20	7.29	7.51
2.80	2.00	3.00	2.32	2.48	3.21	3.01
2.80	2.00	1.95	2.32	2.48	4.81	4.60
2.80	2.00	1.05	2.32	2.48	7.85	8.59
2.80	2.00	0.450	2.32	2.48	18.1	20.0
4.20	1.02	3.00	3.12	2.10	7.12	6.39
4.20	1.02	1.95	3.12	2.10	9.81	9.83
4.20	1.02	1.05	3.12	2.10	18.2	18.3
4.20	1.02	0.450	3.12	2.10	41.6	42.6
4.20	2.01	3.00	3.42	2.79	5.18	4.92
4.20	2.01	1.95	3.42	2.79	7.31	7.58
4.20	2.01	1.05	3.42	2.79	13.4	14.1
4.20	2.01	0.450	3.42	2.79	33.3	32.8
4.20	3.51	3.00	3.72	3.99	3.10	3.34
4.20	3.51	1.95	3.72	3.99	5.50	5.14
4.20	3.51	1.05	3.72	3.99	9.21	9.54
4.20	3.51	0.450	3.72	3.99	24.8	22.2

[a] Solutions contain (7.04–7.27) × 10^{-4} M 3-methylascorbic acid, and observations are at 580 nm; the concentrations are the initial (i) stoichiometric values and the final (f) values after correction for hydrolysis of iron(III). [b] Rate constants calculated from initial rates determined from slopes of absorbance–time plots.

Scheme III

$$Fe(OH_2)^{3+} + 3\text{-MeAsH} \underset{}{\overset{K_f}{\rightleftharpoons}} Fe^{III}(3\text{-MeAs})^{2+} + H_3O^+$$

$$Fe^{III}(3\text{-MeAs})^{2+} \underset{k_{-5}}{\overset{k_5}{\rightleftharpoons}} \{I\bullet\} + Fe^{II}$$

$$\{I\bullet\} \xrightarrow{k_6} Fe^{II} + \text{Org. Product}$$

through a column of Dowex 50W-X12(H^+) resin did not induce any change in the CD spectrum of 3-MeAsH.

The organic products of the oxidation, at concentrations similar to those in the rest of this study, were investigated by ^{13}C NMR after removing the iron(II) and (III) by ion exchange and concentrating the solutions by vacuum distillation as described in the Experimental Section. A test of the procedure on the iron(III) oxidation of ascorbic acid revealed that the major product after 24 h is bicyclic dehydroascorbic acid (**6**) which decomposed to **8** after one week in acidic solution.

The much slower reaction of 3-MeAsH with iron(III) required that the first product spectrum could only be recorded 48 h after starting the reaction, and even then the reaction is only about 80–85% complete. Thus the product spectrum is complicated by unreacted 3-MeAsH and by oxidized decomposition products. The 3-methyl derivative of **6** was identified primarily by analogy to the ascorbic acid system and shows the C3 carbon shifted by 2 ppm and the OCH_3 at 52.2 ppm. A signal a 162.2 ppm appears to be due to the decarboxylation product of the 3-methyl derivative of **8**, but signals due to **8** were too weak to be clearly assigned. Essentially similar results were obtained when the reaction was done in the presence of air. The reaction is about 25% faster because iron(II) is reoxidized to iron(III), but removal of iron(III) by ion exchange is more difficult, apparently because it is complexed by oxidation products.

The assignment of the 3-methyl derivative of **6** was investigated further using the much faster oxidation of 3-MeAsH with I_3^-, which allows the spectra to be recorded within 17 h. This product also shows the OCH_3 signal at 52.2 ppm, while methanol gives a signal at 49.8 ppm under our acidity and concentration conditions. It is concluded that the OCH_3 group survives the oxidation by both iron(III) and I_3^- and the major product is the 3-methyl derivative of **6**.

The oxidation of 3-MeAsH by aqueous iron(III) is strongly inhibited by iron(II). The kinetics have been studied by measuring initial rates with iron(II) added in pseudo-first-order excess and by studying full absorbance–time profiles with iron(II) added at concentrations similar to that of 3-MeAsH and with no added iron(II). For both of the latter conditions, it should be possible to model the data by numerical integration.

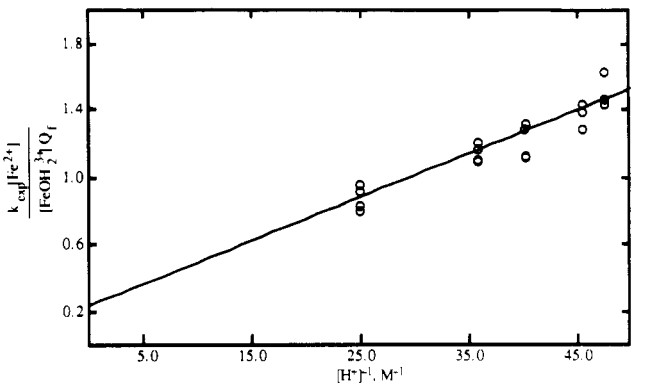

Figure 1. Variation of rate constants from initial rates for the oxidation of 3-MeAsH by aqueous iron(III) as predicted by eq 3.

The initial rate data with a pseudo-first-order excess of iron(II) are consistent with the pseudo-first-order rate constant given by

$$k_{obsd} = \frac{(k_{ox} + K_m k_{ox}'[H^+]^{-1})}{([Fe(II)])}[Fe(OH_2)_6^{3+}]\left\{\frac{K_f[Fe(OH_2)_6^{3+}]}{[H^+] + K_f[Fe(OH_2)_6^{3+}]}\right\} \quad (2)$$

so that

$$\frac{k_{obsd}[Fe(II)]}{[Fe(OH_2)_6^{3+}]Q_f} = k_{ox} + K_m k_{ox}'[H^+]^{-1} \quad (3)$$

where Q_f is the term in braces in eq 2, and k_{ox} and k_{ox}' are rate constant coefficients for paths involving oxidation by $Fe(OH_2)_6^{3+}$ and $Fe(OH_2)_5(OH)^{2+}$, respectively. The plot predicted by eq 3 is shown in Figure 1. Least-squares analysis of these results gives k_{ox} = (2.3 ± 1.2) × 10^{-5} and k_{ox}' = (1.55 ± 0.4) × 10^{-3} M^{-1} s^{-1}. The observed and calculated values are compared in Table II.

The observed rate law and previous experience with ascorbic acid would lead one to expect that the system could be described by the general reaction mechanism in Scheme III. The species $\{I^\bullet\}$ is a radical intermediate, and the exact nature of the k_5 and k_6 steps is left unspecified for the moment. Scheme III predicts the pseudo-first-order rate constant given by eq 4, if the K_f step is a rapid preequilibrium and a steady state is assumed for $\{I^\bullet\}$. This equation is consistent with the observations (eq 2) if k_6/k_{-5}

$$k_{obsd} = \frac{\left(\frac{k_5k_6}{k_{-5}}\right)}{\left([Fe(II)] + \frac{k_6}{k_{-5}}\right)} \left\{\frac{K_f[Fe(OH_2)_6^{3+}]}{[H^+] + K_f[Fe(OH_2)_6^{3+}]}\right\} \quad (4)$$

has an upper limit defined by $[Fe(II)] \geq 4.5 \times 10^{-3}$ M $\gg k_6/k_{-5}$ for these experiments. The overall iron(III) and $[H^+]^{-1}$ dependencies indicate that $Fe(OH_2)_5(OH)^{2+}$ and $Fe(OH_2)_6^{3+}$ are oxidants in either the k_5 or k_6 steps.

For several runs with a pseudo-first-order excess of iron(II), the full course of the reaction was monitored and the absorbance–time variations are given in Figure 2. These graphs show that the iron(III), iron(II), and H^+ dependence is as predicted from eq 3 for the full course of the reaction. These runs give $k_{ox} = 2.2 \times 10^{-5}$ and $k_{ox}' = 1.6 \times 10^{-3}$, in good agreement with the initial rates results.

It should be possible to determine if the iron(III) oxidant is involved in either the k_5 or k_6 steps by determining the iron(III) dependence of k_6/k_{-5} with $[Fe(II)] \leq k_6/k_{-5}$. This was attempted by monitoring the disappearance of the violet color under second-order conditions with either no Fe(II) added initially or Fe(II) added at the same level as the 3-MeAsH. Then the absorbance change was modeled by numerically integrating the differential equations derived from Scheme III. Although straightforward in practice, this approach was a complete failure because the reaction under second-order conditions is much faster than predicted by the parameters derived by eq 3. The problem is illustrated for runs with 4.89×10^{-4} and 9.78×10^{-4} M initial Fe(II) in Figure 3 where the calculated curves are for $k_6/k_{-5} = 1 \times 10^{-6} \ll [Fe(II)]$, which makes the calculated decay as fast as possible. The calculated curve still decays much too slowly, and the disagreement is even worse for runs with no Fe(II) added initially. Clearly something else is happening at low Fe(II) concentrations.

There are several possible explanations for the failure of the high Fe(II) data to predict the low Fe(II) results. One is that the stoichiometry changes so that each ascorbate oxidation produces less than 2 Fe(II) at low initial Fe(II) concentrations. This seems unlikely because the stoichiometry was studied with no Fe(II) added initially and was found to be 1:2. Even so, a model which even supposes that no Fe(II) is produced will not reproduce the data in Figure 3. Another possibility is that Fe(II) is being oxidized, perhaps by O_2, during the runs, although our experience is that this reaction is too slow to be a complication. Nevertheless, two runs were done under identical conditions except that one was anaerobic in an argon atmosphere and the other was exposed to air throughout the run. These two runs gave indistinguishable absorbance–time profiles as shown in Figure 4.

After an exhaustive examination of the absorbance–time profiles for runs with no added Fe(II), we have come to the conclusion that they required an $[Fe(II)]^{-2}$ dependence in the initial stages. Such a dependence has been observed previously for the oxidation of 1,2-dihydroxybenzoic acid,[22] where it was ascribed to formation of a moderately, stable complex of iron(III) and the oxidized organic product involving the carboxylate group. However, for such a mechanism, an $[Fe(II)]^{-1}$ dependence with high added Fe(II) will not simplify to an $[Fe(II)]^{-2}$ dependence at low Fe(II) concentrations. For the latter to happen, there must be parallel reaction pathways so that the $[Fe(II)]^{-2}$ dependent pathway becomes too small to contribute at high Fe(II) concentrations.

One possible source of parallel reactions is that the radical produced in the k_5 step of Scheme III is an iron(III) complex which may react reversibly with iron(III) to give Fe(II) and another iron(III) complex which then decomposes to product. In the second pathway, the initial radical complex might undergo some irreversible change, such as hydration or cyclization, to produce a different iron(III)–radical complex which in turn decomposes by intramolecular electron transfer to Fe(II) and organic product. For ascorbate, the one-electron oxidation product can

(22) Xu, J.; Jordan, R. B. *Inorg. Chem.* **1988**, *27*, 4563.

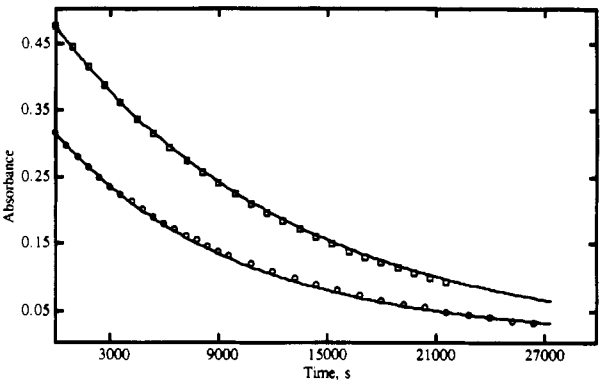

Figure 2. Absorbance–time profiles for the oxidation of 3-MeAsH by aqueous iron(III) in the presence of a pseudo-first-order excess of iron(II): (○) 0.0218 M $Fe(OH_2)_6^{3+}$, 0.0249 M H^+, 0.0105 M iron(II), and 7.05×10^{-4} M 3-MeAsH; (□) 0.0325 M $Fe(OH_2)_6^{3+}$, 0.0211 M H^+, 0.0300 M iron(II), and 7.07×10^{-4} M 3-MeAsH. Curves are calculated from eq 4 with parameters given in the text.

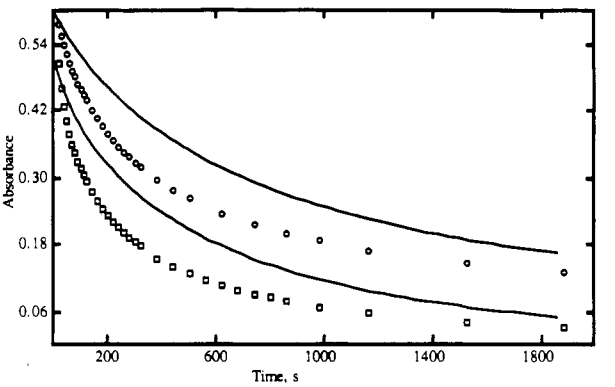

Figure 3. Absorbance–time profiles for the oxidation of 3-MeAsH by aqueous iron(III) for runs containing initial [Fe(II)] of 4.89×10^{-4} M (□) and 9.78×10^{-4} M (○) and otherwise identical with 7.03×10^{-4} M 3-MeAsH, 4.20×10^{-2} M iron(III), and 1.02×10^{-2} M $HClO_4$. The calculated curves are based on parameters determined from initial rates at much higher Fe(II) concentrations (eq 3).

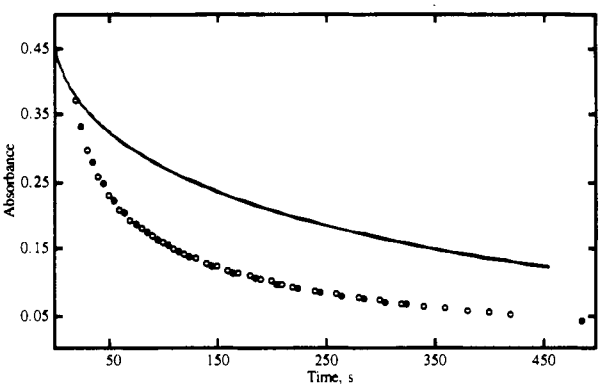

Figure 4. Absorbance–time profile for the oxidation of 3-MeAsH by aqueous iron(III) under aerobic (○) and anaerobic conditions (●) with 7.05×10^{-4} M 3-MeAsH, 4.20×10^{-2} M iron(III), and 1.02×10^{-2} M $HClO_4$. The calculated curves are based on parameters determined from initial rates with a pseudo-first-order excess of Fe(II) concentrations (eq 3).

easily lose a proton to form the semiquinone radical as shown in eq 5, but the methyl group will prevent semiquinone formation

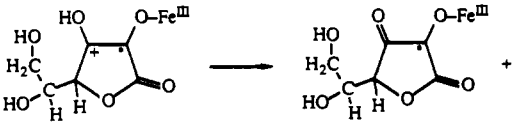

(5)

in 3-MeAsH and hydration and/or cyclization would be probable fates of the radical, in addition to further oxidation.

Scheme IV

$$Fe^{III} + Fe^{III}(3\text{-MeAs})^{2+} \underset{k_{-5}}{\overset{k_5}{\rightleftharpoons}} \{Fe^{III}(3\text{-MeAs}^{\bullet})\}^{3+} + Fe^{II}$$

$$Fe^{III} + \{Fe^{III}(3\text{-MeAs}^{\bullet})\}^{3+} \underset{k_{-7}}{\overset{k_7}{\rightleftharpoons}} \{Fe^{III}(3\text{-MeOxd})\}^{4+} + Fe^{II}$$

$$\{Fe^{III}(3\text{-MeOxd})\}^{4+} \xrightarrow{k_8} Fe^{III} + \text{Product(1)}$$

$$\{Fe^{III}(3\text{-MeAs}^{\bullet})\}^{3+} \xrightarrow{k_9} \{Fe^{III}(3\text{-MeAs}^{\bullet\bullet})\}^{3+}$$

$$\{Fe^{III}(3\text{-MeAs}^{\bullet\bullet})\}^{3+} \xrightarrow{k_{10}} Fe^{III} + \text{Product(2)}$$

A mechanism incorporating these ideas is shown in Scheme IV, where k_9 is the irreversible change of the initial radical intermediate, and 3-MeOxd represents the fully oxidized form of 3-MeAsH without specifying a particular molecular structure. If a steady state is assumed for the intermediates in braces then the rate of total product formation is given by

$$\text{rate} = \left\{k_5[Fe^{III}][Fe(3\text{-MeAs})^{2+}]\left[\left(\frac{k_7}{k_{-5}}\right)\left(\frac{k_8}{k_{-7}}\right)[Fe^{III}] + \left(\frac{k_9}{k_{-5}}\right)[Fe^{II}] + \left(\frac{k_9}{k_{-5}}\right)\left(\frac{k_8}{k_{-7}}\right)\right]\right\} \Big/ \left\{[Fe^{II}]^2 + \left(\frac{k_8}{k_{-7}} + \frac{k_9}{k_{-5}}\right)[Fe^{II}] + \left(\frac{k_8}{k_{-7}}\right)\left(\frac{k_9}{k_{-5}}\right) + \left(\frac{k_8}{k_{-7}}\right)\left(\frac{k_7}{k_{-5}}\right)[Fe^{III}]\right\} \quad (6)$$

This equation indicates that the kinetic behavior is controlled by k_5 and three rate constant ratios. Fortunately, some of the required information can be obtained from the limiting form of eq 6 at high $[Fe^{II}]$ which is given by

$$\text{rate} = \frac{k_5\left(\frac{k_9}{k_{-5}}\right)[Fe^{III}][Fe(3\text{-MeAs})^{2+}]}{[Fe^{II}] + \left(\frac{k_8}{k_{-7}} + \frac{k_9}{k_{-5}}\right)} \quad (7)$$

The results at high $[Fe^{II}]$ indicate that the second term in the denominator is $<4.5 \times 10^{-3}$ and give a numerical expression for $k_5(k_9/k_{-5})$ as described by the right-hand side of eq 3. It is also helpful to note that the limiting form of eq 6 for very low $[Fe^{II}]$ [at the start when no Fe(II) is added] is given by

$$\text{rate} = k_5[Fe^{III}][Fe(3\text{-MeAs})^{2+}] \quad (8)$$

from which it can be seen that this region can define k_5.

The kinetic runs under second-order conditions in $[Fe^{II}]$ and [3-MeAsH] have been fitted graphically to eq 6 by numerical integration. It is found that this model successfully fits the data for the available range of conditions with the following values:

$$\left(\frac{k_9}{k_{-5}}\right) = 2.5 \times 10^{-5} \qquad \left(\frac{k_8}{k_{-7}}\right) = 1.4 \times 10^{-4}$$

$$\left(\frac{k_7}{k_{-5}}\right) = 1.2 \times 10^{-2}$$

Representative fits of the data are shown in Figures 5–7. The model is clearly successful in predicting the dependence of the rate on the concentrations of H^+, Fe(III), Fe(II), and 3-MeAsH. It is difficult to estimate the uncertainties in these parameters, but overall experience with the graphical fits under various conditions indicates a conservative estimate is ±30%.

A final problem is whether the reactions in Scheme IV can be translated into some rational scheme of chemical structures. One possibility is suggested in Scheme V. The one electron oxidation product is shown in various resonance forms in braces to provide a rationale for the parallel pathways. This scheme is simplified by the assumption that intermediates with a carbonium ion at C3 only undergo cyclization in preference to hydration, but various hydrates are possible. The scheme is also based on the idea that dissociation of Fe(III) from the oxidized intermediates, which is expected to occur on the millisecond time scale, will be slow relative to the lifetime of the intermediates due to redox processes.

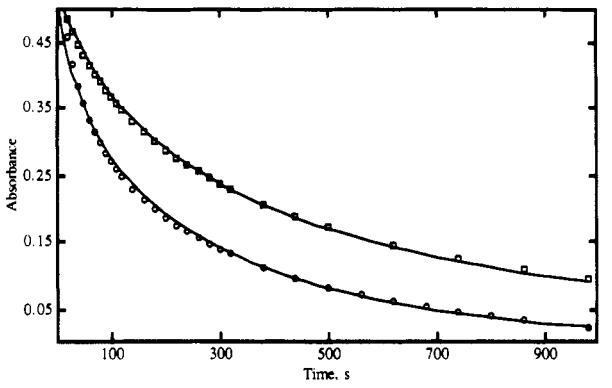

Figure 5. Absorbance–time profile for the oxidation of 3-MeAsH by aqueous iron(III); calculated curves are based on Scheme IV, with parameters given in the text. The solutions contain initial [Fe(II)] of 4.89×10^{-4} M (□) and 9.78×10^{-4} M (○) and are otherwise identical with 7.03×10^{-4} M 3-MeAsH, 4.20×10^{-2} M iron(III), and 1.02×10^{-2} M $HClO_4$. The equilibrium concentrations are 3.12×10^{-2} M $Fe(OH_2)_6^{3+}$ and 2.10×10^{-2} M H^+.

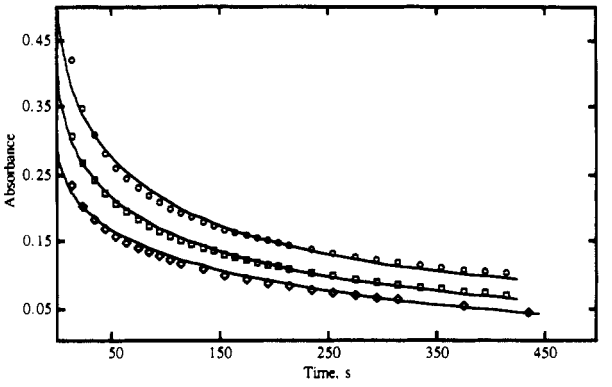

Figure 6. Absorbance–time profile for the oxidation of 3-MeAsH by aqueous iron(III) for conditions with no initial iron(II). The initial conditions are (○) 3.12×10^{-2} M $Fe(OH_2)_6^{3+}$, 2.10×10^{-2} M H^+, and 7.07×10^{-4} M 3-MeAsH; (□) 3.42×10^{-2} M $Fe(OH_2)_6^{3+}$, 2.78×10^{-2} M H^+, and 7.16×10^{-4} M 3-MeAsH; (◇) 2.32×10^{-2} M $Fe(OH_2)_6^{3+}$, 2.49×10^{-2} M H^+, and 7.05×10^{-4} M 3-MeAsH. The curves have been displaced vertically for clarity of presentation.

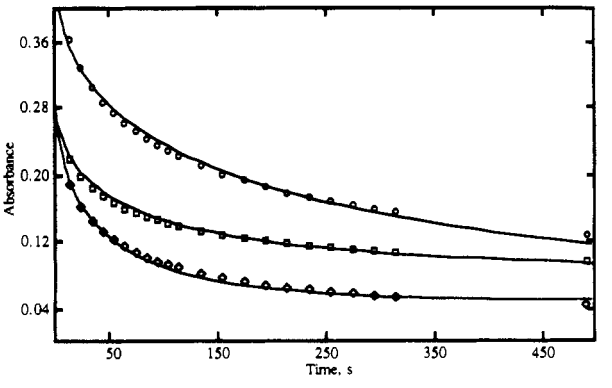

Figure 7. Absorbance–time profile for the oxidation of 3-MeAsH by aqueous iron(III) for conditions with no initial iron(II). The initial conditions are (○) 2.07×10^{-2} M $Fe(OH_2)_6^{3+}$, 1.74×10^{-2} M H^+, and 6.97×10^{-4} M 3-MeAsH; (□) 2.07×10^{-2} M $Fe(OH_2)_6^{3+}$, 1.74×10^{-2} M H^+, and 3.49×10^{-4} M 3-MeAsH; (◇) 3.12×10^{-2} M $Fe(OH_2)_6^{3+}$, 2.10×10^{-2} M H^+, and 3.49×10^{-4} M 3-MeAsH. The curves have been displaced vertically for clarity of presentation.

From eq 7, it can be seen that the value of k_9/k_{-5} and the results at high Fe(II) concentrations can be combined to calculate the specific rate constants for the initial electron transfer (k_5) with $Fe(OH_2)_6^{3+}$ and $(H_2O)_5FeOH^{2+}$ of 0.88 and 64 M^{-1} s^{-1}, respectively. It is noteworthy that the ratio of these rate constants of 1.4×10^{-2} is similar to the value of 2.7×10^{-2} obtained for

Scheme V

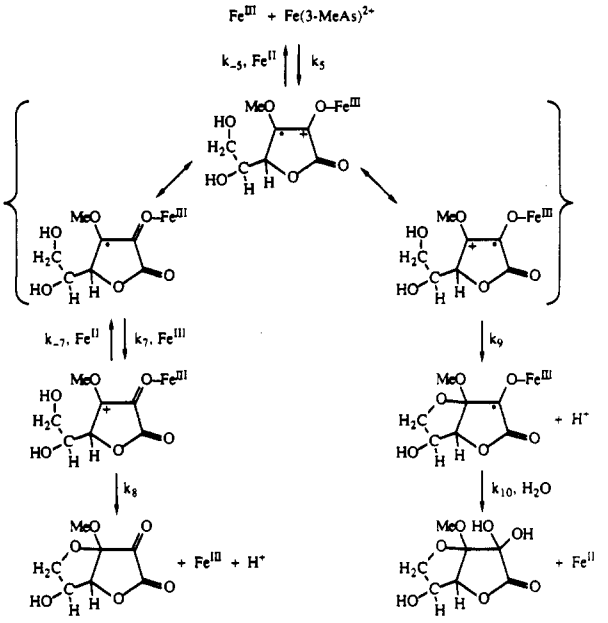

the ascorbic acid system.[1] The higher reactivity of $(H_2O)_5FeOH^{2+}$ was also observed in the 1,2-dihydroxybenzoic acid system[22] where it was ascribed to a substitution controlled inner-sphere reaction. This explanation has also been adopted in a recent study[18] of the iron(III)–ascorbic acid system at higher acidities in excess ascorbic acid.

An assessment of the rate constant ratios suffers from the lack of obvious precedents. From two of these ratios, one can calculate that the proposed cyclization reactions have $k_9/k_8 = 18$. It seems reasonable that the values should be similar and that k_9 is larger because the radical cation reactant may be a higher energy species than the cation in the k_8 step. Perhaps the most surprising observation is that the oxidized intermediates are apparently rapidly reduced by Fe(II) (k_{-5} and k_{-7}), although this must be the case from the simple observation of the strong Fe(II) inhibition. If k_8 and k_9 are of the order of 10^3 s^{-1}, then k_{-5} and k_{-7} must be in the range of 10^8 M^{-1} s^{-1}.

Experimental Section

Materials. Solutions of lithium perchlorate, perchloric acid, and iron(III) perchlorate were prepared and standardized as described previously.[20]

The 3-methyl ascorbic acid was prepared by the method of Shrihatti and Nair[23] by reaction of diazomethane with ascorbic acid in ether. The product was purified by chromatography on Merck Silica Gel-60 (230–400 mesh) with Skelly B (commercial grade *n*-hexane) and increasing amounts of acetone. The product elutes with 45% acetone in Skelly B, and only fractions which have a single TLC spot were collected. More concentrated fractions yielded needles after overnight refrigeration. Other fractions were evaporated to dryness and the product was recrystallized from acetone–hexane to give an overall yield of 50–60% of product with a melting point of 122–123 °C. The UV spectrum of 3-MeAsH in 0.02 M aqueous $HClO_4$ has a maximum at 243 nm (ϵ, 9.73 × 10^3 M^{-1} cm^{-1}) in good agreement with previous reports.[14,24] The ^1H NMR spectrum (300 MHz, DMSO-d_6) agrees with that reported by Shrihatti and Nair,[23] but not with that given by Bryan et al.[25] The proton-decoupled ^{13}C NMR spectrum agrees with that quoted by Paukstelis et al.[24] and is very similar to that of ascorbic acid except for the OCH_3 at 60.2 ppm (in 0.012 M $HClO_4$ H_2O/D_2O relative to internal dioxane at 67.4 ppm).

Oxidation Products. With iron(III) as the oxidant, reactant solutions typically contained 4.2 × 10^{-2} M iron(III) and 1.0 × 10^{-2} M reductant in 5.0 × 10^{-2} M $HClO_4$, and the reaction time was 10 min with ascorbic acid and 24 h with 3-MeAsH. Then the solution was passed through Dowex 50W-X12 (Na^+) to remove the iron species, acidified to pH 2 with $HClO_4$, and reduced in volume about 3-fold by vacuum evaporation to give a sample suitable for NMR analysis. With I_3^- as the oxidant, a stoichiometric amount of oxidant was used, the reaction time was 14 h for 3-MeAsH, and the ion exchange and evaporation steps were omitted.

The products were assigned on the basis of their ^{13}C NMR spectra by comparison to previously reported results.[6,10,12,26] In all cases, the major products identified were monomeric bicyclic dehydroascorbic acid (MBDA) and its decomposition product, diketogulonic acid. The MBDA derivatives from ascorbic acid and 3-MeAsH are primarily distinguished by a resonance at 52.2 ppm in the latter which is assigned to the OCH_3 group.

Instrumentation. The electronic spectra were recorded on a Hewlett-Packard 8451 diode array spectrophotometer for the equilibrium measurements and a Cary 219 for the oxidation kinetics. The complex formation was studied on a Tritech Dynamic Instruments system described previously.[20]

Numerical Analysis. The least-squares and numerical integration methods have been described previously.[20]

Acknowledgment. We thank the Natural Sciences and Engineering Research Council of Canada for financial support and Dr. O. Hindsgaul and Mr. G. Alton for advice and assistance with the preparation of 3-methylascorbic acid.

(23) Shrihatti, V. R.; Nair, P. M. *Indian J. Chem.* **1977**, *15B*, 861.
(24) Paukstelis, J. V.; Mueller, D. D.; Seib, P. A.; Lillard, D. W., Jr. In *Ascorbic Acid: Chemistry, Metabolism and Uses*; Seib, P. A., Tolbert, B. M., Eds.; Advances in Chemistry Series, Vol. 200, American Chemical Society: Washington, DC, 1982; pp 125–151.
(25) Bryan, D. M.; Pell, S. D.; Kumar, R.; Clarke, M. J.; Rodriguez, V.; Sherban, M.; Charkoudian, J. *J. Am. Chem. Soc.* **1988**, *110*, 1498.
(26) Pfeilsticker, K.; Marx, F.; Bockisch, M. *Carbohydr. Res.* **1975**, *45*, 269.